



MODIFICATION OF THE KINETIC PARAMETERS OF *SnSe* BY TERBIUM DOPING

T.A. Jafarov¹,  O.M. Gasanov¹, Kh.A. Adgezalova¹, H.A. Aslanov¹,  J.I. Huseynov^{1*},  I.I. Abbasov²,
R.Sh. Ragimov³

¹Azerbaijan State Pedagogical University, AZ-1000, Baku, Uz. Hajibeyli Str. 68, Azerbaijan

²Azerbaijan State Oil and Industry University, Az-1010, Baku, Azadliq Avenue 20, Azerbaijan

³Baku State University, AZ-1148, Baku, Zahid Xalilov Str. 23, Azerbaijan

*Corresponding Author email: jahangirhuseynov1958@gmail.com

Received August 31, 2025; revised October 31, 2025; accepted November 6, 2025

The kinetic parameters of solid solutions $Tb_xSn_{1-x}Se$ ($0 \leq x \leq 0.05$), grown by the Bridgman method, were investigated at 300 K. It was found that doping with Tb significantly affects the electrical conductivity, Hall coefficient, Seebeck coefficient (thermoelectric power), thermal conductivity, and the concentration and mobility of charge carriers. At low Tb concentrations, a transition from p-type to n-type conductivity is observed, accompanied by a non-monotonic change in the Hall coefficient and the sign of the Seebeck coefficient. Electrical and thermal conductivities decrease due to enhanced scattering at defects caused by introducing Tb. The obtained data are important for controlling the properties of SnSe in its thermoelectric applications.

Keywords: Solid solutions; Kinetic parameters; Doping; Thermoelectric properties; Seebeck coefficient; Electrical conductivity; Thermal conductivity; Carrier concentration; Conductivity type transition

PACS: 71.20.Nr, 72.20.Pa, 61.72.-y

1. INTRODUCTION

Tin selenide (*SnSe*) is a binary semiconductor compound with an orthorhombic (*Pnma*) layered structure, characterized by pronounced anisotropy, low thermal conductivity, and high thermoelectric performance. The presence of Sn atom vacancies in the crystal lattice results in p-type conductivity [1–3].

Due to its high Seebeck coefficient, low thermal conductivity, and sufficient electrical conductivity, *SnSe* is considered one of the best thermoelectric materials, especially in single-crystal form ($ZT \approx 2.6 - 2.8$ at ~ 900 K). Its bandgap width (0.9 – 1.3 eV) also makes it promising for optoelectronic applications. The ease of mechanical cleavage further supports the use of *SnSe* in flexible electronics [4–6].

The material consists of non-toxic and non-deficient elements, which is important from both environmental and economic perspectives. The properties of *SnSe* can be effectively tuned through doping and cation substitution. The introduction of elements such as Na, Ag, and K (for p-type) or Bi, Cl, and I (for n-type) allows control over the charge carrier concentration. Substituting Sn with Pb, Ge, Mn, Co, and other cations affects the structure and functional properties, including reduced thermal conductivity and the emergence of new properties [7–10].

Particular interest lies in doping with rare-earth elements (e.g., La, Ce, Gd), which enhance conductivity and reduce thermal conductivity due to local lattice distortions [11–13]. Among them, terbium (Tb) is especially promising; its ions can act as donors, increasing the electron concentration and promoting n-type behavior. Substituting Sn with Tb also enhances phonon scattering, reduces thermal conductivity, and may introduce localized energy levels [14]. This study investigates the effect of Tb content on the key kinetic parameters of $Tb_xSn_{1-x}Se$ alloys at a temperature of 300 K.

2. EXPERIMENTAL SECTION

For the synthesis of $Tb_xSn_{1-x}Se$ alloys, high-purity starting materials were used: tin of grade B4-000, selenium of grade OC417-4, and chemically pure terbium (99.98%). The synthesis was performed in evacuated quartz ampoules at a pressure of 0.1333 Pa using a two-step direct melting method. In the first stage, the ampoules containing the weighed components were heated at a rate of 4 – 5 °C/min to the melting point of selenium and held at that temperature for 3 – 4 hours. Subsequently, the temperature was gradually increased to 950 – 1000 °C (depending on the composition) and maintained for 8 – 9 hours [15].

The interaction in the *SnSe* – *TbSe* system was investigated using differential thermal analysis (DTA), X-ray diffraction (XRD), microstructural analysis (MSA), as well as measurements of microhardness and density [16]. DTA was conducted using a PerkinElmer Simultaneous Thermal Analyzer STA 6000 (USA) to determine the thermal effects and phase transitions of the synthesized samples. Nitrogen was used as the purge gas at a flow rate of 20 mL/s, and the samples were heated to their melting temperatures at a rate of 5 °C/min.

X-ray diffraction analysis was performed using a Rigaku Miniflex diffractometer operating at 30 kV and 10 mA with $CuK\alpha$ radiation ($\lambda = 1.5406$ Å). Diffraction peaks were recorded over a 2θ range of 0 – 80°. The surface

morphology and microstructure of the samples were examined using a JEOL JSM-6610LV scanning electron microscope (Japan).

Electrical conductivity and the Hall coefficient were measured under direct current conditions in a constant magnetic field using an electromagnet setup [17]. The Seebeck coefficient and thermal conductivity were determined using a fully stationary method, as described in [18]. The experimental uncertainty did not exceed 4.2%.

3. RESULTS AND DISCUSSION

3.1. Physicochemical Analysis

The thermograms of the alloys in the $Tb_xSn_{1-x}Se$ system show sharp peaks during heating and cooling, which correspond to the melting and solidification temperatures, indicating the formation of congruently melting alloys. In the $SnSe$ compound, partial substitution of Sn with Tb lowers the melting temperature due to the incorporation of larger rare-earth (RE) ions, which distort the crystal lattice and weaken interatomic bonds. This leads to structural defects and an additional decrease in melting temperature. The microhardness of samples with $TbSe$ content up to 0.05 mol.% remains at the level of ~ 500 MPa.

Analysis of the intensity of X -ray reflections shows that the sample has a preferred crystal orientation and consists of a single phase. Indexing of the X -ray patterns indicate an orthorhombic crystal system with the space group $D_{2h}^{16} - Pcmn$ (Fig. 1). In the range $0 \leq x \leq 0.05$, no shift in diffraction lines is observed; only their intensity changes, which indicates the formation of solid solutions based on $SnSe$. When Sn atoms are partially replaced with RE atoms of larger ionic radius, the intensity of reflections decreases, and the lattice parameters increase additively. The increase in parameters is linear, with no deviations from Vegard's law observed.

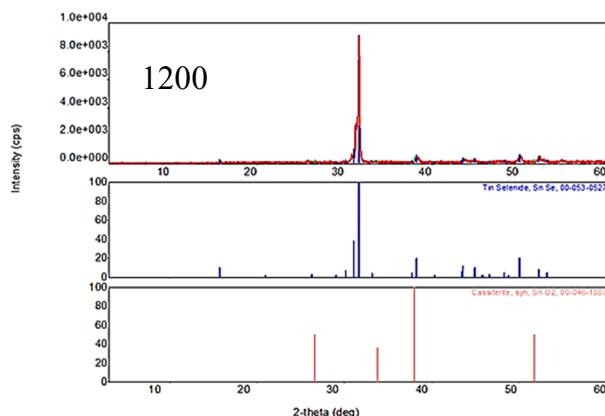


Figure 1. X-ray diffraction spectrum of crystals $Tb_xSn_{1-x}Se$: $x=0.0025$. Below are X-ray diffraction patterns of $SnSe$ and SnO for comparison

X -ray structural analysis shows that the addition of terbium selenides leads to an increase in the unit cell parameters of $SnSe$ as the concentration of Tb increases. This is accompanied by intense charge-carrier scattering due to lattice distortion, consistent with the low thermal conductivity of the alloys [16]. At the same time, the density of the $Tb_xSn_{1-x}Se$ system remains practically unchanged, indicating interstitial positioning of Tb atoms and the formation of Frenkel-type defects [19].

The increase in lattice parameters, the coherent substitution of Sn with Tb , and adherence to Vegard's law confirm the formation of a substitutional solid solution based on $SnSe$. X -ray structural analysis and

pycnometry revealed that the solubility range of $TbSe$ in $SnSe$ at room temperature is limited to 2 mol. %.

Comprehensive physicochemical analysis showed that the $Tb_xSn_{1-x}Se$ system alloys, like $SnSe$, crystallize in an orthorhombic crystal system. With an increase in $TbSe$ content, the lattice parameters, density, and microhardness increase slightly, while the thermal effects shift to lower temperatures. Due to differences in the electronic configuration of Sn and Tb , substitution in the $Tb_xSn_{1-x}Se$ solid solution leads to distortions in the $SnSe$ crystal lattice, while preserving its basic structure.

Atomic force microscopy of the surface topography of $Tb_xSn_{1-x}Se$ crystals revealed that the natural surface is inhomogeneous and has a roughness of about 25 nm. This is due to the presence of weak van der Waals forces between the layers, which lead to the formation of atomic clusters upon cleavage, giving the surface an uneven appearance. X -ray microanalysis revealed the phase composition and element distribution (Fig. 2). The surface was generally homogeneous; however, an excess of selenium was observed within the homogeneity range of $SnSe$.

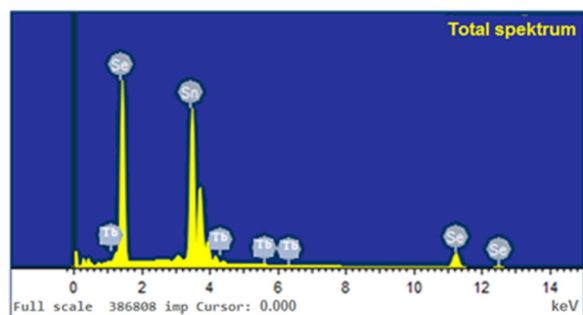


Figure 2. X-ray microanalysis of the crystal surface $Tb_xSn_{1-x}Se$: ($x=0.005$)

Element	Weight %	Atomic %
Sn L	59.69	49.72
Se L	39.90	50.03
Tb L	0.41	0.25
Total	100	100

3.2. Electrophysical and Thermal Properties of $Tb_xSn_{1-x}Se$ Alloys at Various Tb Concentrations

In the solid solution range of ($0 \leq x \leq 0.05$), several kinetic parameters were investigated at room temperature (300 K) for $TbSe$ – containing samples grown by the Bridgman method. These parameters include electrical conductivity (σ), Hall coefficient (R), thermopower (S), thermal conductivity coefficient (k), charge carrier concentration (p, n), and Hall mobility (μ). The obtained results are summarized in Table 1.

$SnSe$ is typically a p –type semiconductor, and its charge transport properties are highly sensitive to doping. As seen from Table 1, with increasing $TbSe$ content in $Tb_xSn_{1-x}Se$ alloys, the resistivity and Hall coefficient increase, while the carrier concentration and mobility decrease.

In the binary compound $SnSe$, with partial cation-cation substitution of Sn atoms by Tb atoms at room temperature ($T = 300$ K), the Hall coefficient (R) strongly depends on the percentage of Tb atoms and varies non-monotonically. This non-monotonic change in the absolute value of the Hall coefficient is explained by the competition of two or more mechanisms depending on impurity concentration.

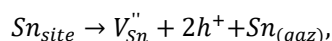
The $SnSe$ compound, in the absence of doping impurities, consistently exhibits p-type conductivity, which has been confirmed both by experimental measurements and quantum-chemical calculations [20, 21]. The primary reason for this is the presence of intrinsic defects in the crystal lattice—primarily tin cation vacancies (V_{Sn}), which act as acceptor centers and promote hole generation.

The formation of such vacancies can be explained in terms of the atomic properties and electronic structure of $SnSe$. First, tin (Sn) has a relatively low ionization energy (first ionization energy ~ 7.34 eV [22]), which facilitates the loss of valence electrons and the transition of Sn atoms to the Sn^{2+} ionic state. Second, selenium (Se), with its high electronegativity (2.55 on the Pauling scale [20]), strongly attracts electrons from the $Sn - Se$ covalent bond, thereby further polarizing and weakening this bond. As a result, Sn cations become less stable in the lattice, especially under Se –rich synthesis conditions, which promotes the formation of cation vacancies

Table 1. The main kinetic parameters of $Tb_xSn_{1-x}Se$ alloys at $T = 300$ K

Composition, x , mol%	R , cm^3/K	S , $\mu V/K$	σ , $\Omega^{-1} \cdot cm^{-1}$	$k \times 10^{-5}$, $W/(m \cdot K)$	μ , $cm^2/(V \cdot s)$	$p(n) \times 10^{17}$, cm^{-3}
0.00	+8.68	+420	18	20	156	7.2
0.10	+25.7	+275	2.42	18	60.5	2.43
0.20	+32.3	+128	0.45	17	14.5	1.93
0.25	-180	-325	0.027	16.4	4.86	0.347
0.50	-1750	-298	0.012	14.5	21.12	0.036
1.00	-1260	-297	0.0063	12.5	6.50	0.05
1.5	-1040	-278	0.0061	12	6.34	0.06
2.00	-898	-262	0.006	11.8	5.39	0.07
2.5	-420	-258	0.012	11.2	5.04	0.15
3.00	-245	-250	0.028	10.7	6.86	0.26
3.5	-176	-246	0.035	9.9	6.16	0.36
4.00	-70	-235	0.04	9	2.82	0.89
4.5	-54	-227	0.043	11.3	2.3	1.16
5.00	-41.6	-210	0.047	14.5	3	1.5

From the standpoint of modern defect thermodynamics, the formation of a cation vacancy in $SnSe$ under thermodynamic equilibrium can be described by the reaction:



where V_{Sn}'' is a doubly negatively charged Sn cation vacancy and h^+ denotes a hole (positive charge carrier) [23]. Such a defect type is thermodynamically stable under slight deviations from stoichiometry, particularly in the case of a tin deficit [19]. These holes can move freely, thus ensuring p-type conductivity [20]. Consequently, the formation of vacancies is accompanied by an increase in the hole concentration that determines the p-type conduction.

Density Functional Theory (DFT) calculations confirm that the formation energy of Sn cation vacancies is significantly lower than that of other intrinsic defects (such as Se vacancies or antisite defects), especially under Se –rich conditions [20]. This indicates the thermodynamic preference for such defects, consistent with p-type conductivity.

In binary $SnSe$, partial cation–cation substitution of Sn by Tb atoms lead to strong dependence of the Hall coefficient (R) on the Tb concentration at room temperature ($T = 300$ K), with a non-monotonic variation (Fig. 3). The non-monotonic change in the absolute value of the Hall coefficient can be explained by the competition of two or more mechanisms depending on the impurity concentration.

At low Tb concentrations, the Hall coefficient is positive, indicating dominant hole-type conduction. As the Tb concentration increases in $Sn_{1-x}Tb_xSe$ alloys, the increase of R_H from +8.68 to +32.3 cm^3/C reflects a decrease in carrier concentration and possible formation of acceptor levels due to the substitution of Sn^{2+} by Tb^{3+} . The sharp sign reversal from positive to negative at 0.25 mol% Tb indicates an inversion of conduction type from hole to electron

conduction. This may be attributed either to the transition of *Tb* from acceptor to donor behavior or to band structure modifications that generate effective electron states.

During cation substitution, *Tb* atoms, according to their electronic configuration ($1s^2 2s^2 2p^6 3s^2 3p^6 4s^2 3d^{10} 4p^6 5s^2 4d^{10} 5p^6 6s^2 4f^9$), act as donors. At low *Tb* concentrations, partial substitution of Sn^{2+} ions by Tb^{3+} introduces donor electrons. These donors compensate part of the holes, thereby neutralizing them. At low impurity levels, compensation starts and the charge carrier concentration decreases [24]. As a result, although the overall hole concentration decreases ($x \leq 0.002$), holes remain the dominant carriers. The compensation of holes leads to an increase in the positive value of the Hall coefficient.

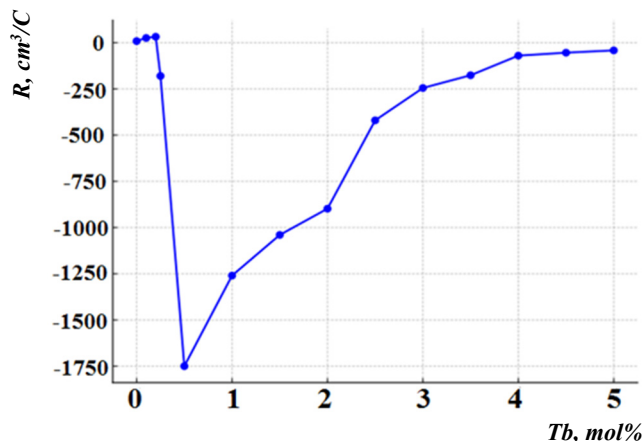


Figure 3. Composition dependence of the Hall coefficient of $\text{Tb}_x\text{Sn}_{1-x}\text{Se}$ system alloys

However, at a critical impurity concentration ($x \approx 0.002 - 0.0025$), donor electrons fully compensate holes, reducing the net carrier concentration to nearly zero (the compensation point). This represents a typical conductivity-type transformation in semiconductors, and the corresponding composition can be characterized as the compensation point. Near this transition, the electron concentration approaches that of holes ($p \approx n$), indicating maximum compensation.

At the inversion point of conductivity type (transition from hole to electron conduction), the Hall coefficient R_H is described by the two-carrier model, since both electrons and holes are present and contribute competitively. The generalized expression for the Hall coefficient in a two-carrier system is:

$$R_H = \frac{p\mu_p^2 - n\mu_n^2}{e(p\mu_p + n\mu_n)^2},$$

where p – is the hole concentration, n – is the electron concentration, μ_p and μ_n are the mobilities of holes and electrons, respectively, and e – is the elementary charge [25]. At the inversion point, the condition $p\mu_p^2 = n\mu_n^2$ is satisfied, and $R_H = 0$. When $p\mu_p^2 < n\mu_n^2$, R_H becomes negative, indicating electron dominance.

Thus, the observed sign reversal and sharp increase in the absolute value of the Hall coefficient at $x = 0.0025$ (0.25 mol%) in $\text{Tb}_x\text{Sn}_{1-x}\text{Se}$ alloys is a key transition point in the electronic structure of the material. The transition to negative values demonstrates a shift to electron-type conduction, showing that *Tb* acts effectively as a donor, introducing electrons into the conduction band [13].

At the composition corresponding to $x = 0.0025$, the sign of the Hall coefficient becomes negative, and its absolute value sharply increases, reaching approximately $-1750 \text{ cm}^3/\text{C}$, indicating a sudden change in the dominant charge carriers from holes to electrons. With further increase in dopant content, the hole carriers are compensated, and then electrons begin to dominate, resulting in a change in the Hall coefficient's sign from positive to negative. The change in conductivity type, i.e., the transition from p – to n – type, is explained by the substitution of Sn^{2+} ions with Tb^{3+} ions, which leads to the generation of additional electrons and the dominance of donor-type defects in the system. Consequently, p – type conductivity transforms into n – type, causing a sharp change in the alloy's electrophysical properties [26]. Such transition points are of particular significance in terms of controlling the functional properties of materials and open up possibilities for their tuning in future applications.

With increasing terbium (*Tb*) content, the absolute value of the Hall coefficient decreases, while its sign remains negative across the entire concentration range, indicating the predominance of electrons as the main charge carriers. In the concentration range $0.0025 < x < 0.025$, the Hall coefficient decreases especially sharply. This is presumably due to the effective donor action of *Tb*, which significantly increases the concentration of free electrons.

As the *Tb* content further increases ($x > 0.025$), the decrease slows down. This behavior may be due to donor state saturation, where further introduction of *Tb* no longer leads to a significant increase in carrier concentration. Additionally, enhanced scattering effects or the formation of localized states may occur, reducing carrier mobility and thereby stabilizing the Hall coefficient value [27].

As shown in the table, the carrier concentration (P) initially decreases from $7.2 \times 10^{17} \text{ cm}^{-3}$ to a minimum value of about $0.036 \times 10^{17} \text{ cm}^{-3}$ at $0.5 \text{ mol}\%$, indicating carrier compensation due to charge capture or the formation of recombination centers. With further increase in Tb content, the carrier concentration rises, reaching $1.5 \times 10^{17} \text{ cm}^{-3}$ at $5 \text{ mol}\%$. This indicates a shift in the role of Tb in the material – from a compensator to a donor capable of generating free electrons in the conduction band [27].

As seen from the table, the carrier concentration (p) decreases from $7.2 \times 10^{17} \text{ cm}^{-3}$ to a minimum value of approximately $0.036 \times 10^{17} \text{ cm}^{-3}$ with the initial introduction of Tb up to $0.5 \text{ mol}\%$, indicating compensation of carriers due to charge trapping or the formation of recombination centers. With a further increase in Tb content, the carrier concentration rises, reaching $1.5 \times 10^{17} \text{ cm}^{-3}$ at $5 \text{ mol}\%$. This indicates a change in the role of Tb in the material – from a compensator to a donor capable of generating free electrons in the conduction band [28].

For pure SnSe at room temperature, the Seebeck coefficient lies in the range of $S \approx +400$ to $+500 \mu\text{V/K}$ (in the table, this value is approximately $+420 \mu\text{V/K}$). Such a high value is attributed to the low carrier concentration and to an anomalous density-of-states function at the energy levels. As the temperature increases, the Seebeck coefficient in SnSe rises, reaching values around $600 - 800 \mu\text{V/K}$ at elevated temperatures ($500 - 800 \text{ K}$) [29]. These characteristics highlight the high potential of SnSe as a thermoelectric converter at elevated temperatures. The combination of these properties gives this material a leading position among high-efficiency thermoelectric materials.

With an increase in terbium content in solid solutions of $Tb_x\text{Sn}_{1-x}\text{Se}$, the Seebeck coefficient (S) initially decreases sharply and then, after crossing into negative values, becomes relatively stabilized (see Fig. 4). In the initial region ($0 \leq x \leq 0.002 \text{ mol}\%$), a rapid decrease in the positive Seebeck coefficient is observed—from $+420 \mu\text{V/K}$ to $+128 \mu\text{V/K}$. This indicates a reduction in the contribution of positive charge carriers (holes) to the thermoelectromotive force. This decrease is explained by the partial substitution of Sn^{2+} ions with Tb^{3+} ions, leading to the emergence of a donor effect and the formation of additional electronic states contributing to the generation of electrons in the conduction band. This partial substitution disrupts the crystal lattice's symmetry, enhances carrier scattering, and thus reduces their transport efficiency.

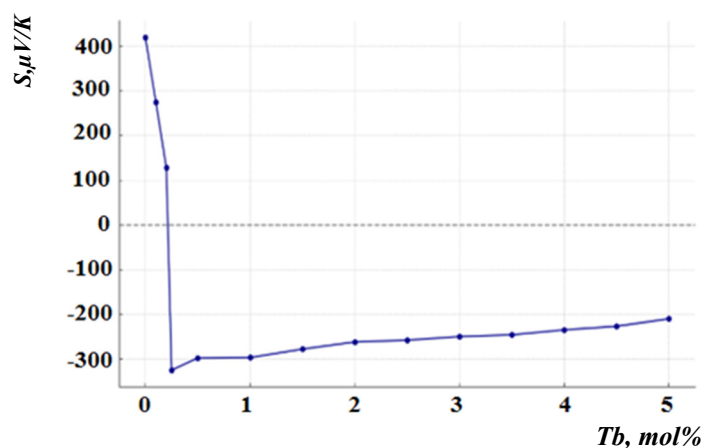


Figure 4. Composition dependence of the Seebeck coefficient of $Tb_x\text{Sn}_{1-x}\text{Se}$ system alloys $\text{Sn}_{1-x}\text{Tb}_x$

In the narrow interval of $0.002 < x < 0.0025 \text{ mol}\%$ Tb , a sign inversion of the Seebeck coefficient is observed: its value changes from $+128 \mu\text{V/K}$ to $-325 \mu\text{V/K}$, indicating a change in the dominant type of charge carriers – from hole-type (p -type) to electron-type (n -type) conductivity. This is associated with reaching a critical concentration of Tb at which the Fermi level shifts close to the conduction band, and electrons become the predominant carriers [30]. Terbium atoms create localized energy levels near the conduction band, which are easily ionized and participate in electron transport.

After the change in conductivity type, in the range of $0.0025 < x < 0.015 \text{ mol}\%$ Tb , the Seebeck coefficient stabilizes in the negative region. This indicates the formation of a new carrier balance dominated by electrons, saturation of the Tb donor levels, stabilization of the energy structure, and an increase in the material's homogeneity.

In the interval of $0.02 < x < 0.05 \text{ mol}\%$ Tb , a gradual decrease in the absolute value of the Seebeck coefficient is observed, which is caused by an increase in free electron concentration, reducing the chemical potential gradient – the main factor determining the thermoelectromotive force. Possible interactions between Tb atoms that lead to electron localization or changes in their effective mass, as well as the ordering of bulk defects in the crystal lattice due to the elevated Tb content, also contribute to the reduction in thermoelectric voltage [31].

As shown in Figure 5, the dependence of the electrical conductivity of $Tb_x\text{Sn}_{1-x}\text{Se}$ solid solutions on the Tb content exhibits a non-monotonic character based on experimental data. According to the presented table, at $x = 0$, the system's electrical conductivity is high, amounting to $\sigma = 18 \Omega^{-1} \cdot \text{cm}^{-1}$. However, with an increase in Tb concentration from 0.1 to $2 \text{ mol}\%$, the conductivity sharply decreases, reaching a minimum value ($\sigma \approx 0.006 \Omega^{-1} \cdot \text{cm}^{-1}$). This effect

is consistent with the literature data [32], which indicate that the introduction of Tb^{3+} ions into the $SnSe$ lattice leads to distortions in the crystal structure, the formation of local energy levels and recombination centers, thereby reducing the concentration of free charge carriers and, consequently, the electrical conductivity.

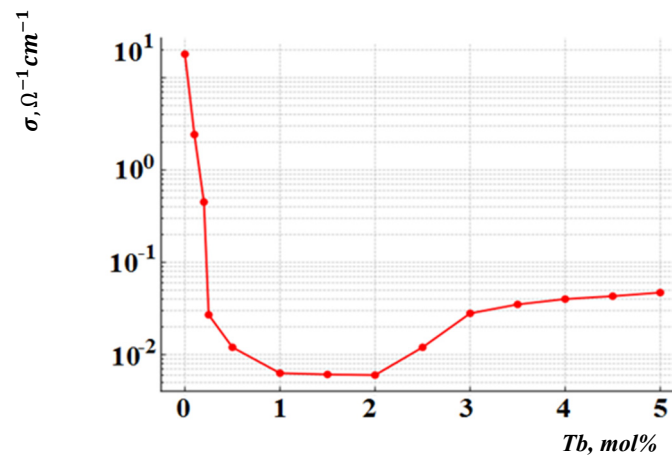


Figure 5. Composition dependence of the specific electrical conductivity of $Tb_xSn_{1-x}Se$ system alloys

This process is explained by the occurrence of lattice distortions due to the incorporation of Tb^{3+} ions into the $SnSe$ crystal lattice, the appearance of localized energy levels, and increased scattering of charge carriers. The difference in valence between Tb and Sn ions ($Tb^{3+} \rightarrow Sn^{2+}$) leads to the formation of compensation and recombination centers in the system, which in turn reduces the concentration of free charge carriers [17].

With a further increase in Tb content above 2 mol. %, the electrical conductivity begins to gradually increase. This growth can be explained by the formation of additional conductive levels in the energy band after reaching the critical concentration of Tb atoms, the manifestation of the percolation effect, and the weakening of the degree of carrier localization. Thus, the mobility of charge carriers in the system is partially restored, resulting in an increase in electrical conductivity.

These observations indicate that the electrical conductivity in the $Tb_xSn_{1-x}Se$ system significantly depends not only on the number of free carriers but also on their energy state and scattering processes within the crystal structure. Such non-monotonic dependence is typically explained by the localization-delocalization transition, structural distortions, and percolation theory.

The study of the dependence of the alloys' thermal conductivity on the terbium (Tb) content revealed that as the Tb concentration increases from 0 to 4.0 mol%, the material's thermal conductivity gradually decreases—from $20 \times 10^{-5} \text{ W/(m} \cdot \text{K)}$ to $9 \times 10^{-5} \text{ W/(m} \cdot \text{K)}$. However, with further increases in Tb concentration, the opposite trend is observed—thermal conductivity rises to $14.5 \times 10^{-5} \text{ W/(m} \cdot \text{K)}$ at 5.0 mol%. This behavior can be explained by changes in the alloy's microstructure. At the initial stage of Tb incorporation, impurity atoms distort the crystal lattice due to differences in atomic radii and mass, which enhances phonon scattering—the main carriers of heat in solids. Moreover, increasing Tb concentration leads to a higher number of point defects and disorder, further hindering heat transport. These effects account for the observed decrease in thermal conductivity [33].

When the threshold concentration ($\sim 4 \text{ mol\%}$) is exceeded, it is likely that a new phase or an ordered structure forms, in which the level of phonon scattering decreases. This may be associated with a phase transition accompanied by structural stabilization and a reduction in defect density. As a result, an increase in thermal conductivity is observed despite the continued increase in Tb content [34]. The obtained data indicate a complex dependence of thermal conductivity on alloy composition, driven by the competition between phonon scattering at defects and structural rearrangement of the material at high Tb concentrations.

The dependence of the Hall mobility of free carriers on Tb concentration in the alloys is distinctly nonlinear. As the Tb content increases from 0 to $\sim 2.5 \text{ mol\%}$, there is a sharp decrease in mobility, attributed to enhanced scattering of charge carriers at lattice defects introduced by Tb atoms. Terbium atoms, differing in size and valence, induce distortions in the crystal lattice and promote the formation of localized states that serve as effective scattering centers. Additionally, the possible formation of traps associated with $Tb 4f$ —electron levels also contributes to reduced mobility. At higher concentrations (2.5 – 4.5 mol%), the character of the dependence becomes more complex: fluctuations are observed, likely due to Tb atom clustering, secondary phase formation, or changes in the charge transport mechanism [35]. Magnetic scattering associated with local magnetic moments of Tb may also play a role. Thus, the reduction in mobility with increasing Tb concentration is determined by a complex interplay of structural, electronic, and magnetic factors.

In summary, doping $SnSe$ with terbium leads to complex changes in thermal and electrical properties, caused by structural and electronic transformations within the system. These results are essential for understanding the

mechanisms of heat and charge transport in doped semiconductors and enable optimization of compositions for thermoelectric and other functional applications.

CONCLUSIONS

The study demonstrated that doping the SnSe semiconductor with terbium (Tb) significantly alters its electronic and thermal properties, thereby altering the mechanisms of charge and heat transport. Depending on the Tb content, phase and functional transitions are observed, including a change in the type of conductivity from p -type to n -type, which is accompanied by a sharp restructuring of kinetic parameters — the Hall coefficient, thermoelectric power (Seebeck coefficient), electrical conductivity, and others.

A charge carrier compensation point has been identified, at which maximum suppression of conductivity occurs — an important characteristic for tuning the functional properties of the material. Doping leads to a significant decrease in thermal conductivity due to enhanced phonon scattering, which is a favorable factor for thermoelectric applications. The observed nonmonotonic dependencies of parameters on Tb concentration are associated with the competition between donor and compensating effects, carrier localization, and structural changes in the crystal lattice.

The obtained results provide a basis for the targeted control of the properties of SnSe-like materials and for optimizing their composition for thermoelectric and sensor applications.

ORCID

✉ O.M. Gasanov, <https://orcid.org/0000-0003-4888-7686>; ✉ J.I. Huseynov, <https://orcid.org/0000-0002-4498-2400>

✉ I.I. Abbasov, <https://orcid.org/0000-0001-8111-2642>

REFERENCE

- [1] A.T. Buruiana, C. Mihai, V. Kuncser, and A. Velea, “Advances in 2D Group IV Monochalcogenides: Synthesis, Properties, and Applications,” *Materials*, **18**(7), 1530 (2025). <https://doi.org/10.3390/ma18071530>
- [2] J. Rundle, and S. Leoni, “Layered Tin Chalcogenides SnS and SnSe: Lattice Thermal Conductivity Benchmarks and Thermoelectric Figure of Merit,” *The Journal of Physical Chemistry C*, **126**(33), 14036–14046, (2022); <https://doi.org/10.1021/acs.jpcc.2c02401>
- [3] J.M. Flitcroft, I. Pallikara, and J. M. Skelton, “Thermoelectric Properties of Pnma and Rocksalt SnS and SnSe,” *Solids*, **3**(1), 155–176 (2022). <https://doi.org/10.3390/solids3010011>
- [4] M. Yadav, V. Singh, S.K. Sharma, *et al.* “Temperature driven n - to p -type conduction switching in SnSe and its mitigation through Zn doping with added advantage of Improved thermoelectric performance,” *Emergent Materials*, **8**, 3753–3760 (2024). <https://doi.org/10.1007/s42247-024-00873-0>
- [5] N. Zakay, A. Schlesinger, U. Argaman, *et al.* “Electrical and Optical Properties of γ -SnSe: A New Ultra-narrow Band Gap Material,” *ACS Applied Materials & Interfaces*, **15**(12), 15668–15675 (2023). <https://doi.org/10.1021/acsami.2c22134>
- [6] M. Kumar, S. Rani, P. Vashishtha, *et al.* “Exploring the optoelectronic properties of SnSe: a new insight,” *Journal of Materials Chemistry C*, **10**, 16714–16722 (2022). <https://doi.org/10.1039/D2TC03799H>
- [7] A.Q. Zhao, B. Qin, D. Wang, Y. Qiu, and L.-D. Zhao, “Realizing High Thermoelectric Performance in Polycrystalline SnSe via Silver Doping and Germanium,” *ACS Appl. Energy Mater.* **3**, 2049–2054 (2020). <https://doi.org/10.1021/acsaem.9b01475>
- [8] A. Duong, V. Nguyen, G. Duvjir, *et al.* “Achieving $ZT=2.2$ with Bi-doped n -type SnSe single crystals,” *Nat Commun*, **7**, 13713 (2016). <https://doi.org/10.1038/ncomms13713>
- [9] Y. Shu, X. Su, H. Xie, *et al.* “Modification of Bulk Heterojunction and Cl Doping for High-Performance Thermoelectric SnSe₂/SnSe Nanocomposites,” *ACS Appl Mater Interfaces*, **10**(18), 15793–15802 (2018). <https://doi.org/10.1021/acsami.8b00524>
- [10] R.Md. Aspan, N. Fatima, R. Mohamed, U. Syafiq, and M.A. Ibrahim, “An Overview of the Strategies for Tin Selenide Advancement in Thermoelectric Application,” *Micromachines*, **12**, 1463 (2021). <https://doi.org/10.3390/mi12121463>
- [11] F. Li, W. Wang, Z.-H. Ge, *et al.* “Enhanced Thermoelectric Properties of Polycrystalline SnSe via LaCl₃ Doping,” *Materials (Basel)*, **11**(2), 203 (2018). <https://doi.org/10.3390/ma11020203>
- [12] Y. Qin, T. Xiong, J.-F. Zhu, *et al.* “Realizing high thermoelectric performance of Cu and Ce co-doped p -type polycrystalline SnSe via inducing nanoprecipitation arrays,” *Journal of Advanced Ceramics*, **11**, 1671–1686 (2022). <https://doi.org/10.1007/s40145-022-0639-6>
- [13] I.I. Abbasov, Sh.S. Ismailov, V.A. Abdurahmanova, *et al.* “Concentration dependences of electrical conductivity and the Hall effect of the $Ce_xSn_{1-x}Se$ single crystals,” *Low Temperature Physics*, **45**, 1277–1280 (2019). <https://doi.org/10.1063/10.0000209>
- [14] J.I. Huseynov, and T.A. Jafarov, “Effect of γ -ray radiation on electrical properties of heat-treated $Tb_xSn_{1-x}Se$ single crystals,” *Semiconductors*, **46**, 430–432 (2012). <https://doi.org/10.1134/S1063782612040082>
- [15] J.I. Huseynov, and T.A. Jafarov, “The Influence of γ -Irradiation on Thermoelectric and Heat Conduction of $Ln_{0.01}Se_{0.99}$ ($Ln = Pr, Tb, Er$) Monocrystals,” *World Journal of Condensed Matter Physics*, **4**(1), 1–5 (2014). <http://dx.doi.org/10.4236/wjcmp.2014.41001>
- [16] I.I. Aliev, M.I. Murguzov, Sh.S. Ismailov, *et al.* “Phase relations and properties of alloys in the SnSe-DySe system,” *Inorg. Mater.* **50**, 237–240 (2014). <https://doi.org/10.1134/S0020168514030029>
- [17] J.I. Huseynov, M.I. Murguzov, and S.S. Ismayilov, “Specific features of self-compensation in $Er_xSn_{1-x}Se$ solid solutions,” *Semiconductors*, **47**, 323–326 (2013). <https://doi.org/10.1134/S106378261303010X>
- [18] J.I. Huseynov, M.I. Murguzov, S.S. Ismayilov, *et al.* “On the thermopower and thermomagnetic properties of $Er_xSn_{1-x}Se$ solid solutions,” *Semiconductors*, **51**, 153–157 (2017). <https://doi.org/10.1134/S1063782617020075>
- [19] J.I. Huseynov, K.A. Hasanov, T.A. Jafarov, and I.I. Abbasov, “Compensating Effect of Terbium Impurity on the Conductivity of $Tb_xSn_{1-x}Se$ Solid Solutions,” *Ukrainian journal of physics*, **65**(3), 225–230 (2020). <https://doi.org/10.15407/ujpe65.3.225>
- [20] Y. Huang, C. Wang, X. Chen, *et al.* “First-principles study on intrinsic defects of SnSe,” *RSC Advances*, (44), 27139 – 27832 (2017). <https://doi.org/10.1039/c7ra03367b>

- [21] S. Gowthamaraju, U.P. Deshpande, S. Anwar, *et al.* "Effect of vacancy on thermoelectric properties of polycrystalline SnSe," *J. Mater. Sci. Mater. Electron.* **32**, 11568–11576 (2021). <https://doi.org/10.1007/s10854-021-05750-8>
- [22] Y. Gong, W. Dou, B. Lu, *et al.* "Divacancy and resonance level enables high thermoelectric performance in n-type SnSe polycrystals," *Nat Commun.* **15**(1), 4231 (2024). <https://doi.org/10.1038/s41467-024-48635-0>
- [23] A.K. Tolloczko, S.J. Zelewski, J. Ziembicki, *et al.* "Photoemission Study of the Thermoelectric Group IV-VI van der Waals Crystals (GeS, SnS, and SnSe)," *Advanced Optical Materials*, **12**(6), 2302049 (2024). <https://doi.org/10.1002/adom.202302049>
- [24] M.R. Shankar, A.N. Prabhu, A.M. Ashok, *et al.* "Role of Bi/Te co-dopants on the thermoelectric properties of SnSepolycrystals: an experimental and theoretical investigation," *Journal of Materials Science*, **59**, 13055–13077 (2024). <https://doi.org/10.1007/s10853-024-09984-9>
- [25] J.E. Dill, C.F.C. Chang, D. Jena, and H.G. Corre, "Two-carrier model-fitting of Hall effect in semiconductors with dual-band occupation: A case study in GaN two-dimensional hole gas," *J. Appl. Phys.* **137**, 025702 (2025). <https://doi.org/10.1063/5.0248998>
- [26] C. Zhang, X.-G. He, H. Chi, *et al.* "Electron and hole contributions to normal-state transport in the superconducting system $\text{Sn}_{1-x}\text{In}_x\text{Te}$," *Phys. Rev. B*, **98**, 054503 (2018). <https://doi.org/10.1103/PhysRevB.98.054503>
- [27] X. Cui, T. Hu, H. Wu, *et al.* "Charge Carrier Transport Behavior and Dielectric Properties of $\text{BaF}_2\text{:Tb}^{3+}$ Nanocrystals," *Nanomaterials*, **10**(1), 155 (2020). <https://doi.org/10.3390/nano10010155>
- [28] I.I. Abbasov, and J.I. Huseynov, "Charge-transfer Processes in $(\text{SnS})_{1-x}(\text{PrS})_x$ Alloys," *Ukr. J. Phys.* **62**(10), 883-888 (2017). <https://doi.org/10.15407/ujpe62.10.088>
- [29] A. Golabek, N.K. Barua, E. Niknam, L.T. Menezes, and H. Kleinke, "Large Improvements in the Thermoelectric Properties of SnSe by Fast Cooling," *Materials*, **18**(2), 358 (2025). <https://doi.org/10.3390/ma18020358>
- [30] K.A. Hasanov, V.V. Dadashova, F.F. Aliyev, *et al.* "Effect of Phonon Drag on the Thermopower in a Parabolic Quantum Well," *Semiconductors*, **50**, 295–298 (2016). <https://doi.org/10.1134/S106378261603009X>
- [31] J.I. Huseynov, M.I. Murquzov, and R.F. Mamedova, "Thermal Conductivity and Termal EMF of Materials for Thermal Energy Converters," in: *TPE-06 3rd Intern. Conf. on Technical and Physical Problems in Power Engineering*, (Ankara, 2008).
- [32] D.I. Huseynov, M.I. Murguzov, and S.S. Ismailov, "Thermal conductivity of $\text{Er}_x\text{Sn}_{1-x}\text{Se}$ ($x \leq 0.025$) solid solutions," *Inorg Mater.* **44**, 467–469 (2008). <https://doi.org/10.1134/S0020168508050063>
- [33] Sh.S. Ismailov, M.A. Musaev, I.I. Abbasov, V.A. Abdurahmanova, *et al.* "Effect of doping level and compensation on thermal conductivity in $\text{Ce}_x\text{Sn}_{1-x}\text{Se}$ solid solutions," *Low Temperature Physics*, **46**, 1114–1120 (2020). <https://doi.org/10.1063/10.0002155>
- [34] C.-W.T. Lo, Sh. Song, Y.-Ch. Tseng, *et al.* "Microstructural Instability and Its Effects on Thermoelectric Properties of SnSe and Na-Doped SnSe," *ACS Appl. Mater. Interfaces*, **16**(37), 49442–49453 (2024). <https://doi.org/10.1021/acsami.4c11319>
- [35] X. He, H. Zhang, T. Nose, *et al.* "Degenerated Hole Doping and Ultra-Low Lattice Thermal Conductivity in Polycrystalline SnSe by Nonequilibrium Isovalent Te Substitution," *Advanced Science*, **9**(13), 2105958 (2022). <https://doi.org/10.1002/advs.202105958>

МОДИФІКАЦІЯ КІНЕТИЧНИХ ПАРАМЕТРІВ SnSe ШЛЯХОМ ЛЕГУВАННЯ ТЕРБІЄМ

Т.А. Джафаров¹, О.М. Гасанов¹, Х.А. Адгезалова¹, Х.А. Асланов¹, Я.І. Хусейнов¹, І.І. Аббасов², Р.Ш. Рагімов³

¹Азербайджанський державний педагогічний університет, AZ-1000, Баку, вул. Уз. Гаджибейлі, 68, Азербайджан

²Азербайджанський державний університет нафти та промисловості, AZ-1010, Баку, проспект Азадлик, 20, Азербайджан

³Бакинський державний університет, AZ-1148, Баку, вул. Західа Халілова, 23, Азербайджан

Кінетичні параметри твердих розчинів $\text{Tb}_x\text{Sn}_{1-x}\text{Se}$ ($0 \leq x \leq 0,05$), вирощених методом Бріджмена, досліджувалися при 300 К. Було виявлено, що легування Tb суттєво впливає на електропровідність, коефіцієнт Холла, коефіцієнт Зеєбека (термоЕРС), теплопровідність, а також концентрацію та рухливість носіїв заряду. При низьких концентраціях Tb спостерігається перехід від р-типу до n-типу провідності, що супроводжується немонотонною зміною коефіцієнта Холла та знака коефіцієнта Зеєбека. Електро- та теплопровідність зменшуються через посилене розсіювання на дефектах, спричинених введенням Tb. Отримані дані важливі для контролю властивостей SnSe в його термоелектричних застосуваннях.

Ключові слова: тверді розчини; кінетичні параметри; легування; термоелектричні властивості; коефіцієнт Зеєбека; електропровідність; теплопровідність; концентрація носіїв; перехід типу провідності